Molecular Conformation and Applicaton of Stereoregular PMMA Langmuir-Blodgett Films

Jang-Joo Kim, Sang-Don Jung and Wol-Yon Hwang

CONTENTS

ABSTRACT

Molecular conformations of stereoregular poly(methyl methacrylate) (PMMA) monolayers have been investigated by scanning probe microscopes. Isotactic and syndiotactic PMMAs were found to have right and left hand helical structures, respectively. On the contrary atactic PMMA showed rather random arrangement of the chains. It has been demonstrated that the PMMA Langmuir-Blodgett (LB) films can be utilized to form nanoscale patterns down to 50 nm and to form a geodesic lens. It has also been manifested that the quantum efficiency of a polymer electroluminescent device can be significantly enhanced by inserting the PMMA LB films between the emitting layer and the cathode. All the applications utilize the unique characteristics of the LB films to form thin and uniform films in the molecular level.

Table 1. Material characteristics of stereoregular PMMAs [5].

Tacticity	Molecular Weight	Poly-dispersity	Contents of Triads (%)			T_g (°C)
			I	H	S	
a-PMMA	185,000	1.05	15	37	48	100
s-PMMA	100,000	1.9	6	10	84	123
i-PMMA	250,000	4.3	97	2	1	51

I. INTRODUCTION

Poly(methyl methacrylate) (PMMA) Langmuir-Blodgett (LB) films are of interest due to their potential application in optical devices and microlithography [1]-[3]. About 30 years ago, different stereoregular PMMAs were found to result in significantly different surface pressure-area (π-A) isotherms [4]. In spite of this earlier work, molecular conformations of stereoregular PMMA monolayers at different surface pressure have not been studied much. In this paper, detailed molecular conformations and applications of stereoregular PMMA LB films will be reported.

II. EXPERIMENTAL

Isotactic (*i*-), syndiotactic (*s*-) and atactic (*a*-) PMMAs were purchased from Polyscience Inc. and used without further purification. Their physical properties and contents of triads are listed in Table 1. They were dissolved in chloroform and the solution was spread on deionized water. A computer controlled normal type polytetrafluoroethylene Langmuir trough was used [6]. The surface pressure and the surface potential were measured using the Wilhelmy plate technique and the vibrating plate method, respectively. The PMMA LB films were transferred onto the highly oriented pyrolytic graphite (HOPG) and mica at the various surface pressures for the investigation of the chain conformation by the scanning tunneling microscopy (STM) and atomic force microscopy (AFM), respectively. Images of the monolayers were taken in the constant height mode under the atmospheric condition for both cases.

III. SURFACE PRESSURE AND SURFACE POTENTIAL OF THE FLOATING MONOLAYERS

The surface potentials and the apparent dipole moments (μ_n) of *a*-, *s*-, and *i*-PMMAs

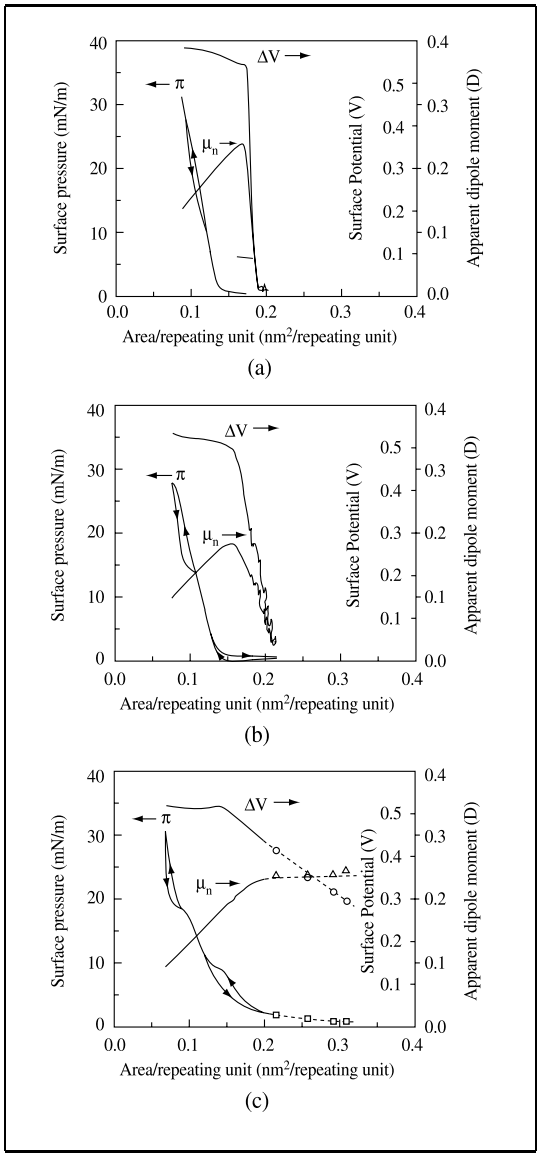

Fig. 1. Surface pressure (π), surface potential (ΔV), and apparent dipole moment (μ_n) - area isotherms for (a) atactic, (b) syndiotactic, and (c) isotactic PMMAs.

are shown in Fig. 1 with surface pressure-area (π-A) isotherms. The π-A isotherms are qualitatively consistent with the previous results [1], [2], [4]. The surface potentials of the *s*- and *a*-PMMAs increase rapidly from zero even in the region where $\pi = 0$. In the high surface concentration region where π increases from 0 to the first inflection point, the surface potentials increase but with lower rate. Eventually, they reach to saturation values when the films were compressed beyond the 1st inflection point. Apparent dipole moments increase rapidly in the region of $\pi = 0$ to reach the maximum at the point where the surface pressure starts to rise and then decrease upon further compression. The maximum μ_n values are 0.17 and 0.23 Debye (D) for *s*- and *a*-PMMAs, respectively.

On the contrary, the surface potential of *i*-PMMA increases monotonically in the region where the surface is lower than the 1st inflection point ($\pi < 8.5$ mNm^{-1}). In the region, the apparent dipole moment is almost constant with 0.23 D. The surface potential above the 1st inflection point shows the similar trend as the *a*- and *s*-PMMAs in the region of $\pi > 0$. The fact that the apparent dipole moment is kept constant in the expanded region implies that the molecular orientation does not change upon compression in the region. The high value of μ_n and the same position of the pendant groups in the *i*-PMMA suggest that the chains have horizontal disposition with the hydrophilic ester groups touching the water surface.

The maximum μ_n values seem to be smaller than the molecular dipole moment of

methyl ester group (1.39 D). In general, the μ_n of a monolayer at the air/water interface estimated from the measured surface potential is smaller than that of the molecular dipole moment. The discrepancy has been explained in terms of the polarization due to water molecules and uncertainties in the value of the relative permittivity [7]. However, the discrepancy is still remained unsolved and only the relative value of μ_n is meaningful in the case of the monolayer at the air/water interface.

IV. MOLECULAR CONFORMATION OF PMMA MONOLAYERS

STM and AFM images of the *i*-PMMA monolayer transferred onto the HOPG at the surface pressure of 15 mNm^{-1} [8], [9] are shown in Fig. 2. The monolayer was transferred during the upward stroke (vertical direction in the images). The AFM image is similar to the STM image, suggesting that STM can be used to obtain molecular images of thin nonconducting polymers even though there are some arguments on the mechanism of the imaging. All the images in Fig. 2 show closely packed well ordered chain arrangement. However details of the images are different for different areas, indicating that the monolayer consists of mixed phases. For instance, the lower part of the image in Fig. 2(a) appears to be coiled in contrast to the upper part of the image where the PMMA chains look linear. The coiled and linear appearance of the chains may represent helical conformation and a horizontal disposition, respectively. The fact that the monolayer is composed of mixed phases is natural since the surface pressure of 15 mNm^{-1} is located between the two inflection points in

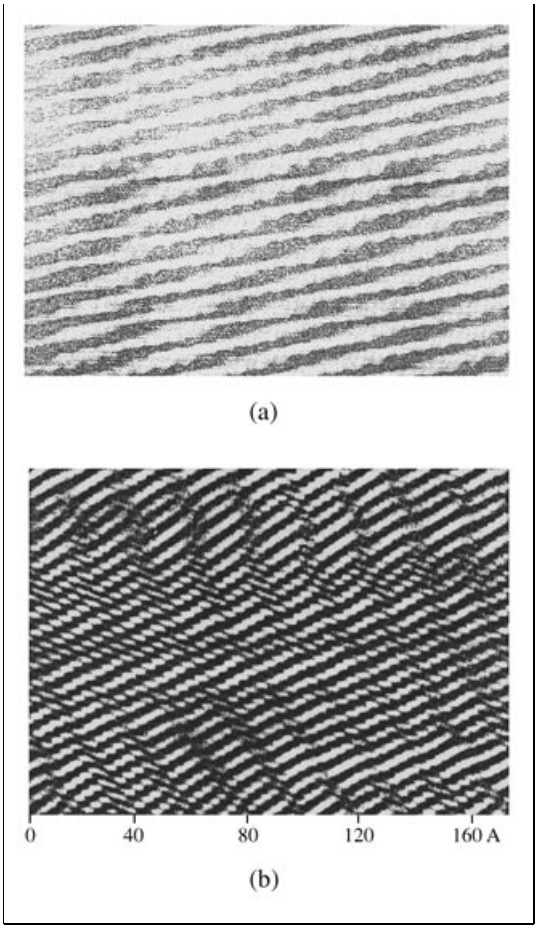

Fig. 2. (a) STM, and (b) AFM images of the isotactic PMMA monolayer transferred at the surface pressure of 15 mN/m^{-1}. The scanning ranges are (a) 10.2 nm × 9.1 nm, and (b) 16.7 nm × 16.6 nm, respectively.

the π-A isotherm. This mixed phase appearance of the images with the linear and coiled parts suggests that the low inflection point is related to the phase transformation from horizontal disposition to the helix. The contrast formed by the pitches of the helices of the chain can be observed in Fig. 2 as a band across the chains. The band appears only in the coiled region. It is interesting to note that the helix is coiled right-handedly which was reproducibly obtained for different samples.

The spacing between the chains and the pitch of the helix were measured by comparing the images of the molecules with the underlying graphite images. The width of the chains varied from sample to sample with an average value of 0.37 nm. The variation was $\pm$0.08 nm. The spacings between chains of the linear parts and the coiled parts are almost the same in the images of mixed phases. The appearance of the helix and the small spacing between the chains indicate that the helix is a single stranded one. The chain spacing of the monolayer is too small for the molecule to have a double strand helical conformation proposed by Brinkhuis and Schouten [10] since the width of the double helix is about 1.25 nm.

Monolayers of *a*- and *s*-PMMA monolayers were transferred at the surface pressure of 10 mNm^{-1}. It was also observed that both monolayers have long range ordered chain arrangement over 10 nm $\times$ 10 nm area [11]. In contrast to the *i*-PMMA, however, the *s*-PMMA monolayer showed left-handed helix and *a*-PMMA rather random side chain arrangement. The reason why different stereoregular PMMAs show different coil handedness is not clear yet. Further experiments are required to clarify the results and for the molecular conformations to be more conclusive.

V. APPLICATIONS

1. Nanoscale Lithography

PMMA LB films have been utilized to form nanostructures [12]. 15 monolayers of atactic PMMA LB films were transferred on the 50 nm thick Cr layer evaporated on Si wafer at the surface pressure of 12 mNm^{-1}. Electron beam (Cambridge EBMF 10.5) was used to form fine patterns. The exposed pattern was developed by the solution of cellulose diluted with methanol by 1:3 for 10 - 20 sec. The developed pattern was transferred to the Cr layer by wet etching. Commercially available CR-7 from Cyantek Co. was used as the Cr etchant. After the stripping of the PMMA layers with acetone, the pattern was examined by scanning electron microscopy. The results are shown in Fig. 3. 15 layers of LB films were thick enough to protect the underlying Cr layers from the etchant suggesting the PMMA LB films are uniform and pinhole free. Fine patterns with 0.1 μm line and spacing were successfully obtained and even 50 nm patterns could be obtained with the PMMA LB films.

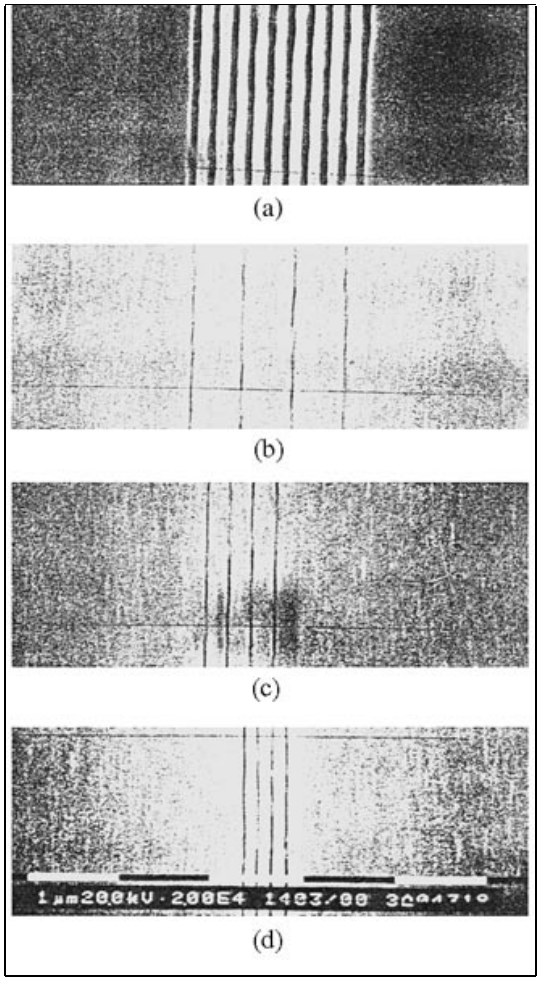

Fig. 3. Scanning electron micrographs of (a) 0.1 μm lines with 0.1 μm spacing, (b) 50 nm lines with 0.5 μm spacing, (c) 50 nm patterns with 0.2 μm spacing, and (d) 50 nm lines with 0.1 μm spacing formed using *a*-PMMA LB films as electron beam resist.

2. Geodesic Lens

When light propagates through a deformed planar waveguide region, it follows the shortest path according to the Fermat's principle. If the guiding plane is deformed properly, it is possible to make a lens called geodesic lens. The lens has application potential in integrated optics because of its large numerical aperture, no chromatic aberration, and mode independent focal length. It is usually fabricated by making a spherical depression on a substrate and forming a guiding layer on the surface by Ti diffusion. LB technique is an another way to form organic planar waveguide on a deformed surface with uniform layer thickness because of the layer-by-layer deposition characteristics. *i*-PMMA was used as waveguide material. The LB film was transferred at the surface pressure of 15 mNm^{-1}. Total 640 layers were transferred to form about 0.64 μm thick waveguide [13]. $LaSF_9$ prism was employed to launch the light (transverse magnetic mode) into the waveguide. The waveguide showed a single mode behavior at 0.6328 μm. The light launched at $\pm$0.5 mm from the lens axis showed clear focusing behavior as shown in Fig. 4. The measured focal lengths agree well with theoretical ones [14].

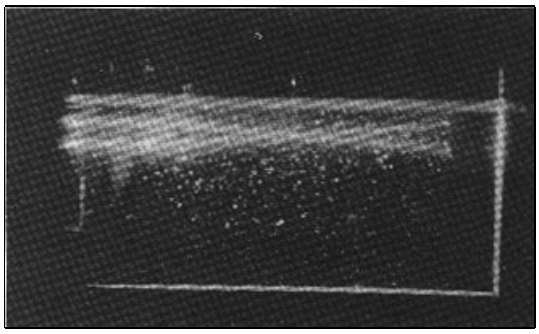

Fig. 4. A geodesic lens formed by *i*-PMMA LB films.

3. Tunneling Barrier to Enhance the Quantum Efficiency in Polymer Light Emitting Diode

Electroluminescence (EL) from conjugated polymers is in active research recently since the first demonstration of it from poly (p-phenylene vinylene) (PPV) [15]. Subsequently, PPV derivatives and other conjugated polymers have been used to achieve increased quantum efficiencies and to provide a range of colors [16]-[21]. Various materials, such as indium-tin-oxide (ITO), semitransparent gold, or polyaniline, can be used as hole injecting electrodes, however ITO has the advantage of high conductivity and high transparency over the visible range combined with high work function for adequate hole injection. Metals such as aluminum, calcium and magnesium-silver have been evaporated on the polymer films to provide the electron injection electrode. In most conjugated polymers, electron injection has proved more difficult than hole injection. To achieve good efficiency it has been necessary to use a low work function metal such as calcium to reduce the barrier to electron injection [22], [23]. Unfortunately, low work function metals are reactive in air environment.

Various methods have been tried to achieve balanced injection of holes and electrons without using the metals having low work function. These include the formation of heterojunction or blending [19] with electron transporting materials and synthesis of new emitting materials having high electron affinity. In this paper we will demonstrate another method to control hole and electron injection by inserting a thin insulating layer between an emitting layer and an electron injecting electrode as shown in Fig. 5. In the device, the effective barrier to electron injection can be lowered while the injection of holes to the emitting layer is reduced if the thickness of the insulating layer is within the tunneling range. As a result, more balanced injection of electrons and holes is expected and the quantum efficiency will increase significantly. *a*-PMMA was used as the insulating material. The material has the energy bandgap of about 6 eV and therefore shows good insulating properties.

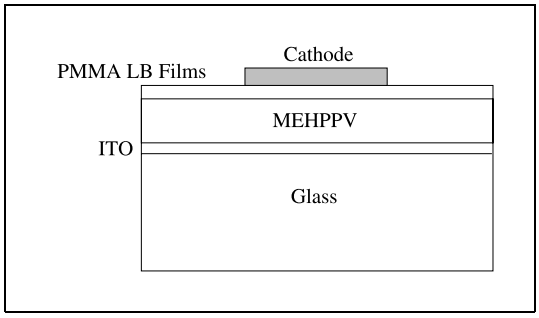

Fig. 5. Schematic diagram of polymer electroluminescence device. MEHPPV is used for the luminescent material.

The devices are formed on glass substrates coated with ITO. A layer of poly[2-methoxy-5-(2-ethylhexyloxy)-1,4-phenylene-vinylene] (MEHPPV) was deposited onto the ITO by spin coating from dichloroethane solution [16]. The thickness of the layer was about 90 nm measured with an Alpha Step profilometer.

After drying at 100 °C for an hour in an oven, *a*-PMMA LB films were transferred onto the emitting layer at the surface pressure of 10 mN/m. The number of the monolayers varied from 2 to 14. Aluminum electrodes were vacuum evaporated onto the upper surface of the PMMA LB films after drying the films in an oven at 100 °C for 1 hour. Light output from the devices was measured using an optical power meter (Newport 835) as a function of the applied field and current. Electroluminescent spectra were measured using a dual grating monochromator (Spex 270M) with the photomultiplier tube (Hamamatsu R955). All the experiments were performed in air and at the room temperature.

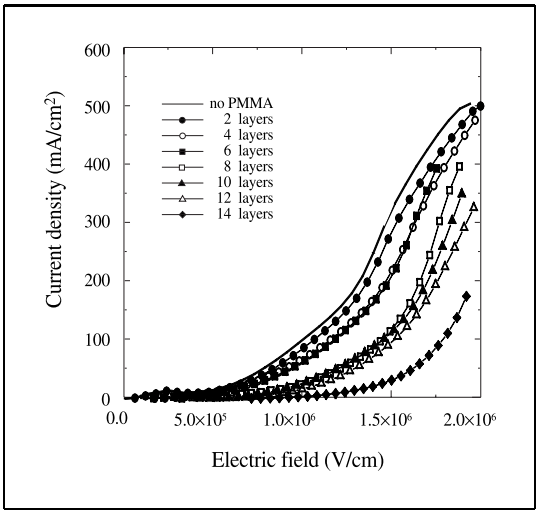

Fig. 6. Current vs. electric field of the EL devices for different thickness of PMMA LB layers: 2 nm (full circle), 4 nm (circle), 6 nm (full square), 8 nm (square), 10 nm (full triangle), 12 nm (triangle), 14 nm (full diamond) and no PMMA LB layers (solid).

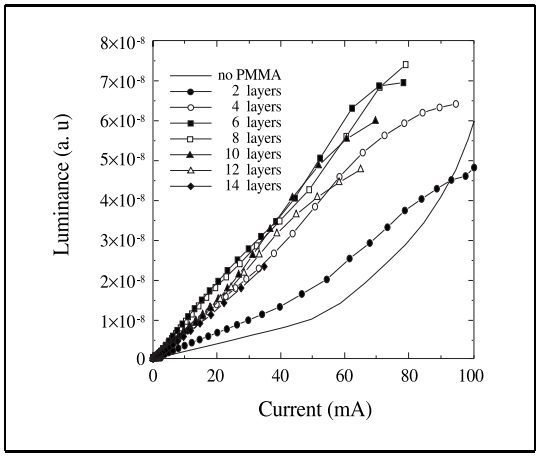

Fig. 7. Luminance vs. current characteristics of the EL devices for different thickness of PMMA LB layers: 2 nm (full circle), 4 nm (circle), 6 nm (full square), 8 nm (square), 10 nm (full triangle), 12 nm (triangle), 14 nm (full diamond) and no PMMA LB layers (solid).

Current-voltage characteristics of the EL devices under forward bias are shown in Fig. 6. The current density at a certain electric field decreases as the number of PMMA LB layers increase. The dependence of the emission intensity on the injected current (L-I) is shown in Fig. 7 for different number of LB layers. As are typical polymer light emitting devices, the emission intensity increases linearly with the injection current for all the devices. The relative quantum efficiency (the slopes in the L-I curves) increases rapidly up to 6 layers and remains or slowly decreases as the number of the layers increase further. The quantum efficiency was enhanced by more than 4 times compared to the MEHPPV only device by inserting the thin insulating layer.

All the behaviors may be explained based on the energy band model (Fig. 8). Major carrier flowing through the device is known to be hole. If we insert the thin insulating layer in the device, it will block the hole transport through the device. As the thickness of the insulating layer is getting thicker, the blocking becomes more effective due to the more effective blocking of the hole tunneling through the LB films, resulting smaller current densities (mainly hole current) under the same applied potential in the device.

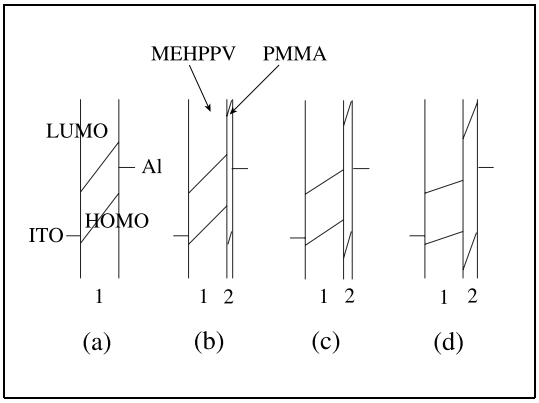

Fig. 8. Schematic energy band model to illustrate the electroluminescence characteristics of the devices: (a) without PMMA LB layers, (b) 2 nm, (c) 6-8 nm and (d) thicker than 10 nm of PMMA LB layers. 1 and 2 represent MEHPPV and PMMA layers, respectively.

In contrast to the hole injection, inserting the thin insulating layer between the emitting layer and the cathode does not increase the effective barrier to the electron injection as long as the thickness of the layer is within a certain range. If the cathode is in direct contact with the emitting layer (Fig. 8(a)), the energy barrier height to the electron injection is fixed to the difference between the LUMO level of the emitting layer and the metal work function ($\Delta\phi_{em}$). However if we insert a thin insulating layer between the metal and the emitting layer (Fig. 8(b)-(d)), $\Delta\phi_{em}$ changes with applied bias and the thickness of the insulating layer. Because of that, increasing the thickness of the insulating layer has two different effects in terms of electron tunneling probability: One is decreasing the tunneling probability due to the increasing tunneling barrier thickness. The other one is increasing the tunneling probability due to the decreasing $\Delta\phi_{em}$ and also due to the increasing potential drop in the insulating layer. The latter effect may be dominant over the former if the insulating layer is thinner than a certain limit, as notified from the higher luminescence up to 8 layers. If the layer is thicker than the limit, most of the potential drop takes place within the insulating layer. In the case, the insulating layer determines carrier transport through the device and higher electric field should be applied to get a certain electron current density. In our special case the limiting thickness of the PMMA layer turns out to be 8 nm.

The above discussion indicates that more balanced injection of electron and hole is achievable by inserting the thin insulating layer, which leads to the enhancement of the quantum efficiency. The above discussion is based on the assumptions that the major current flowing through the devices is the hole

current and the luminescence efficiency is proportional to the electron current injected into the devices. These assumptions seem to be quite reasonable in our system.

VI. CONCLUSIONS

Molecular conformations of stereoregular PMMA monolayers were investigated by scanning probe microscopes. *i*- and *s*-PMMAs were found to have right and left hand helical structures, respectively. On the contrary *a*-PMMA showed rather random arrangement of the chains. It has been demonstrated that the PMMA LB films can be utilized to form nanoscale patterns down to 50 nm and to form a geodesic lens. It has also been demonstrated that the quantum efficiency of a polymer electroluminescence device can be significantly enhanced by inserting the PMMA LB films between the emitting layer and the cathode. All the applications utilize the unique characteristics of the LB films to form thin and uniform films in the molecular level.

The authors greatly acknowledge Prof. Hong-Ku Shim and Mr. In-Nam Kang for their supply of the light emitting material, Drs. T. Zyung, I-C. Jeon and J.-S. Ha, and Ms. Y.-E. Kim for their help in experiments and Dr. H. Park for helpful discussion. The work was performed with the support from The Ministry of Information and Communication of Korea.

REFERENCES

[1] P. Stroeve, M. P. Srinivasan, B. G. Higgins, and S. T. Kowel, "Langmuir-Blodgett multilayers of polymer-merocyanine-dye mixtures," *Thin Solid Films*, vol. 146, pp. 209-220, 1987.

[2] S. W. J. Kuan, C. W. Frank, C. C. Fu, D. R. Allee, P. Maccagno, and R. F. W. Pease, "Ultrathin polymer films for microlithography," *J. Vac. Sci. Technol.* B, vol. 6, pp. 2274-2279, 1988.

[3] S. W. J. Kuan, C. W. Frank, Y. H. YenLee, T. Eimori, D. R. Allee, R. F. W. Pease, and R. Browning, "Ultrathin poly(methylmethacrylate) resist films for microlithography," *J. Vac. Sci. Technol.* B, vol. 7, pp.1745-1750, 1989.

[4] N. Beredjick and H. E. Ries, Jr., "Differentiation of stereoregular polymethyl methacrylates by the film balance technique," *J. Poly. Sci*., vol. 46, pp. 286-270, 1960.

[5] E. Jhon, "Miscibility of the crystalline and amorphous polymer blends," Ph. D. thesis, Korea Advanced Institute of Science and Technology, 1989.

[6] S.-D. Jung, J.-J. Kim, and C.-K. Choi, "Construction of computer controlled Langmuir trough and its performance test," *Hwahakkonghak*, vol. 32, pp. 325-331, 1994.

[7] O. N. Oliveira, Jr., D. M. Taylor, T. J. Lewis, S. Salvagno, and C. J. M.Stirling, "Estimation of group dipole moments from surface potential measurements on Langmuir monolayers," *J. Chem. Soc., Faraday Trans.*, vol. 85, pp. 1009-1015, 1989.

[8] J.-J. Kim, S.-D. Jung, H.-S. Roh, and J.-S. Ha, "Molecular conformation of isotactic PMMA Langmuir-Blodgett films observed by scanning tunneling microscopy," *Thin Solid Films*, vol. 244, pp. 700-704, 1994.

[9] S.-D. Jung, J.-J. Kim, and I.-C. Jeon, "Helical chain conformation of isotactic PMMA LB films observed by atomic force microscopy," *Synthetic Metals*, vol. 71, pp. 2025-2026, 1995.

[10] R. H. G. Brinkhuis and A. J. Schouten, "Thin-film behavior of poly(methyl methacrylate). 1. Monolayers at the air-water interface," *Macromolecules*, vol. 24, p. 1487, 1991.

[11] J. S. Ha, H.-S. Roh, S.-D. Jung, S.-J. Park, J.-J. Kim, and E.-H. Lee, "Structural study of a poly(methyl methacrylate) Langmuir-Blodgett film on a graphite surface by scanning tunneling microscope," *J. Vac. Sci. Technol*. B, vol. 12, pp. 1977-1980, 1994.

[12] S.-D. Jung, "Langmuir-Blodgett films of stereoregular PMMA: Molecular conformations and application potential as electron beam resists," Ph. D. thesis, Seoul National Univ., 1993.

[13] S.-D. Jung, J.-J. Kim, W.-Y. Hwang, and T. Zyung, "Transfer characteristics of Langmuir-Blodgett films of stereoregular poly(methyl methacrylate)," *Mol. Cryst. Liq. Cryst*., vol. 247, pp. 281-291, 1994.

[14] W.-Y. Hwang, S.-D. Jung, T. Zyung, and J.-J. Kim, "A geodesic PMMA waveguide lens fabricated by Langmuir-Blodgett Technique," *Polymer Preprint*, vol.35, pp.268-269, 1994.

[15] J. H. Burroughes, D. D. C. Bradley, A. R. Brown, R. N. Marks, K. Mackay, R. H. Friend, P. L. Burns, and A. B. Holmes, "Light-emitting diodes based on conjugated polymers," *Nature*, vol. 347, no. 11, pp. 539-541, 1990.

[16] D. Braun and A. J. Heeger, "Visible light emission from semiconducting polymer diodes," *Appl. Phys. Lett*., vol. 58, no. 18, pp. 1982-1984, 1991.

[17] C. Zhang, S. Hoger, K. Pakbaz, F, Wudl, and A. J. Heeger, "Yellow electroluminescent diodes utilizing poly(2,5-bis(cholestanoxy)-1,4-phenylene vinylene)," *J. Electron. Mater*., vol. 22, no. 4, pp. 413-417, 1993.

[18] T. Zyung, D.-H. Hwang, I.-N. Kang, H.-K. Shim, W.-Y. Hwang, and J.-J. Kim, "Novel blue electroluminescent polymers with well-defined conjugation length," *Chem. Mater*., vol. 7, no. 8, pp. 1499-1503, 1995.

[19] I.-N. Kang, D.-H. Hwang, H.-K. Shim, T. Zyung, and J.-J. Kim, *Macromolecules*, to be printed in Feb. 1996.

[20] W. Tachelot, S. Jacobs, H. Ndaykengurukiye, and H. J. Geise, "Blue electroluminescent devices with high quantum efficiency from alkoxy-substituted poly(para-phenylene vinylene)-trimers in a polystyrene matrix," *Appl. Phys. Lett*., vol. 64, no. 18, pp. 2364-2366, 1994.

[21] Z. Yang, I. Sokolik, and F. E. Karasz, "A soluble blue-light-emitting polymer," *Macromolecules*, vol. 26, no. 5, pp. 1188-1190, 1993.

[22] S. Aratani, C. Zhang, K. Pakbaz, S. Hoger, F. Wudle, and A. J. Heeger, "Improved efficiency in polymer light-emitting diodes using air-stable electrodes," *J. Electron. Mater*., vol. 22, no. 7, pp. 745-749, 1994.

[23] I. D. Parker, "Carrier tunneling and device characteristics in polymer light-emitting diodes," *J. Appl. Phys*. vol. 75, no. 3, pp. 1656-1666, 1994.

Jang-Joo Kim graduated Seoul National University in 1977 with B.S. and in 1980 with M.S. degrees from the Chemical Engineering Department, respectively. He continued his academic work at Stanford University in California, USA, getting his Ph.D from the Materials Science and Engineering Department in 1986. After 11/2 years of post doctoral work at SRI International in California, USA, he joined ETRI in 1987 as a Senior Researcher. He is currently a Principal Member of Research Staff and the leader of Organic Materials for Electronics and Photonics Team of the institute. His research area covers nonlinear optical organic materials and devices, organic electroluminescent materials and LED, photorefractive organic materials and organized molecular films (Langmuir-Blodgett films). He has co-authored over 50 papers and holds more than 10 patents in those fields.

Sang-Don Jung for photograph and biography, see this issue, p. 193.

Wol-Yon Hwang was born in Korea on December 12, 1963. He received the B.S. degree in Physics from the Pusan National University, Pusan, Korea, in 1985, and the M.S. and Ph.D. degrees in physics from the Korea Advanced Institute of Science and Technology, Taejon, Korea, in 1987 and 1990, respectively. In 1990, he joined the Research Department of ETRI as a Senior Researcher. His current research interests include electro-optic waveguide modulator/switch and tunable wavelength filter.